

# The fermion spectrum in braneworld collisions

---

Paul.M.Saffin<sup>1\*</sup> and Anders Tranberg<sup>2,3†</sup>

<sup>1</sup>*School of Physics and Astronomy, University of Nottingham  
University Park, Nottingham NG7 2RD, United Kingdom.*

<sup>2</sup>*DAMTP, University of Cambridge  
Wilberforce Road, Cambridge, CB3 0WA, United Kingdom.*

<sup>3</sup>*Department of Physical Sciences, University of Oulu,  
90014 Oulu, Finland.*

ABSTRACT: In braneworld collisions fermions originally localised on one brane can be transferred to another brane, or to a space-time boundary. By modelling branes as scalar field kinks we bounce them off boundaries and study resulting effects according to a braneworld observer. Extending on our previous work, we numerically compute the spectrum of excitations of fermion modes localised on the brane and boundary, in terms of the momentum  $k$  along the brane dimensions. We find that the spectrum depends strongly on collision velocity and fermion-scalar coupling. Also, high-momentum modes tend to “fall off” the kinks and become delocalised radiation.

KEYWORDS: Kinks, fermions, branes.

---

\*email: paul.saffin@nottingham.ac.uk

†email: anders.tranberg@oulu.fi

---

## Contents

<b>1. Introduction</b>	<b>1</b>
<b>2. Scalar-fermion model in 4+1 dimensions</b>	<b>2</b>
2.1 The kink and fermion bound states	3
2.2 The boundary and more fermion bound states	5
2.3 Bogoliubov coefficients	6
2.4 Individual modes	8
<b>3. The fermion spectrum</b>	<b>9</b>
3.1 Large $p$	10
3.1.1 Velocity dependence	11
3.1.2 Coupling dependence	11
<b>4. Conclusion</b>	<b>12</b>

---

## 1. Introduction

In braneworld scenarios our Universe is pictured as a hypersurface living in a higher dimensional spacetime, with our standard model particles bound to the hypersurface. In string theory the natural choice for such hypersurfaces are the D-branes [1], or the boundaries of spacetime [2]. However, the braneworld idea was first proposed in the context of field theory models, using topological defects to construct bound states of scalar fields on their world-volume [3].

In condensed matter systems, it is well known that fermions can be trapped by impurities in the system, in the sense that the lowest energy states are localised around these impurities (see, for instance [4]). In a similar way, topological defects may lead to localised fermion states [5, 6] and one can construct the matter sector of the standard model on such defects [7].<sup>1</sup>

Multiple branes may exist along the extra dimensions, and so it is likely that brane-brane collisions will take place. This has prompted various scenarios for the creation of the cosmic microwave background anisotropies [9], reheating [10] and baryogenesis. In the latter case, the baryon asymmetry is created as the localised fermions carried by the colliding branes are transferred in a CP-asymmetric way.

In [11], we extended the work of [12], studying collisions of branes represented by topological defects in 1+1 dimensional  $\phi^4$  theory (a kink), on which fermions were localised.

---

<sup>1</sup>Note, that there are other dynamical ways of ensuring localisation to the brane, for instance [8].

We found that fermions are indeed transferred in kink-anti-kink collisions, but also when bouncing a kink off a boundary. These boundaries can themselves be thought of as branes [2]. The final state resulting from kink-boundary and kink-kink collisions was rather sensitive to the collision velocity and the scalar-fermion coupling, with an oscillatory rather than monotonic dependence for the number of transferred fermions [12, 11].

In [11, 12], only the zero momentum fermion modes were considered, and we now extend the treatment further by including the bound-states of fermions with non-zero momenta along the brane dimensions. The system we simulate is that of a domain wall in five dimensions colliding with a (parallel) spatial boundary, we are then able to evaluate the particle spectrum of fermions resulting from such a collision, as viewed by braneworld observers on either the brane or boundary.

## 2. Scalar-fermion model in 4+1 dimensions

We will model the brane collisions in terms of kinks of a real scalar field  $\phi$  in 4+1 dimensions. Coupled to this field is a Dirac fermion  $\psi$  which, as we shall see, allows for a bound state localised on the kink; these correspond to the braneworld fields. The action is

$$S_{\text{bulk}} = - \int dt dz d^3x \left[ \frac{1}{2} \partial_\mu \phi \partial^\mu \phi - i \bar{\psi} \gamma^\mu \partial_\mu \psi + \frac{\lambda}{4} (\phi^2 - 1)^2 - ig \phi \bar{\psi} \psi \right], \quad (2.1)$$

to which we add a boundary term

$$S_{\text{boundary}} = - \int dt d^3x \left[ \sqrt{\frac{\lambda}{2}} \left( \frac{1}{3} \phi^3 - \phi \right) - \frac{i}{2} \bar{\psi} \psi \right]_{z=0}. \quad (2.2)$$

For a discussion of this term see [11], [15]. We will use the conventions

$$\eta^{\mu\nu} = \text{diag}(-1, 1, 1, 1, 1), \quad \{\gamma_\mu, \gamma_\nu\} = 2\eta_{\mu\nu}, \quad \bar{\psi} = \psi^\dagger \gamma_0, \quad (2.3)$$

and we have singled out the  $x^5 = z$  direction which will be into the bulk, orthogonal to the 3-dimensional branes, all of which will be assumed to be parallel to each other. In 4+1 dimensional spacetime, the fermions are 4-component complex fields, and we employ the chiral representation, for which

$$\gamma_0 = \begin{pmatrix} 0 & -i \\ -i & 0 \end{pmatrix}, \quad \gamma_J = \begin{pmatrix} 0 & i\sigma^j \\ -i\sigma^j & 0 \end{pmatrix}, \quad \gamma_z = -i\gamma_0\gamma_1\gamma_2\gamma_3 = \begin{pmatrix} -1 & 0 \\ 0 & 1 \end{pmatrix}. \quad (2.4)$$

with  $\sigma^j$  the Pauli matrices. We can then split the spinors as

$$\Psi = \Psi_L + \Psi_R = \begin{pmatrix} \psi_L \\ \psi_R \end{pmatrix}, \quad (2.5)$$

with

$$\Psi_R = \frac{1}{2}(1 + \gamma_z)\Psi, \quad \Psi_L = \frac{1}{2}(1 - \gamma_z)\Psi. \quad (2.6)$$

To match the conventions used in [11], we write

$$\psi_L = \psi_2, \quad \psi_R = i\psi_1. \quad (2.7)$$

where  $\psi_{1,2}$  each have two complex component<sup>2</sup>.

We assume that the scalar field does not depend on the directions  $\underline{x} = x_j$ ,  $j = 1, 2, 3$  along the brane but only on the orthogonal direction  $z$ . In that case, the scalar equation of motion reduces to

$$\ddot{\phi}(t, z) = \partial_z^2 \phi(t, z) - \lambda (\phi^2(t, z) - 1) \phi(t, z), \quad (2.8)$$

whereas for the fermions we have

$$\dot{\psi}_1(t, \underline{x}, z) + \sigma^j \partial_j \psi_1(t, \underline{x}, z) + \partial_z \psi_2(t, \underline{x}, z) - g\phi(t, z)\psi_2(t, \underline{x}, z) = 0, \quad (2.9)$$

$$\dot{\psi}_2(t, \underline{x}, z) - \sigma^j \partial_j \psi_2(t, \underline{x}, z) + \partial_z \psi_1(t, \underline{x}, z) + g\phi(t, z)\psi_1(t, \underline{x}, z) = 0. \quad (2.10)$$

We have neglected the fermion back-reaction  $i g \langle \bar{\Psi} \Psi \rangle$  on the scalar field for reasons of simplification. Our main interest is in the behaviour of the fermions, and in the setup here back-reaction would only lead to a small correction to the kink profile, indeed, the zero modes generate no back-reaction. Of course, in the presence of many fermions, such as in a high-temperature thermal state, such effects cannot be discarded (see [13] on how to deal with this).

## 2.1 The kink and fermion bound states

The static scalar field equation has a kink solution,

$$\phi_K(z) = \tanh\left(\frac{z - z_0}{D}\right), \quad D = \sqrt{\frac{2}{\lambda}}, \quad (2.11)$$

here centered at  $z = z_0$  with width  $D$ . We will operate on the negative half-axis  $z < 0$ , with the kink incident on a boundary at  $z = 0$ .

To solve the fermion equation of motion in the background of the static kink [14, 12], we will use a separable ansatz for the fermion field, and write

$$\psi_1(t, \underline{x}, z) = \mathcal{F}_K(t, z)\chi_1(t, \underline{x}), \quad \psi_2(t, \underline{x}, z) = 0. \quad (2.12)$$

We find that

$$\partial_z \mathcal{F}_K(t, z) + g\phi(t, z)\mathcal{F}_K(t, z) = 0, \quad (2.13)$$

$$\dot{\chi}_1(t, \underline{x}) + \sigma^j \partial_j \chi_1(t, \underline{x}) = 0. \quad (2.14)$$

The  $\mathcal{F}_K$  is a profile function in the  $z$ -direction, and is the term responsible for localizing the fermion on the domain wall,

$$\mathcal{F}_K = \sqrt{\frac{\Gamma[gD + \frac{1}{2}]}{2D\sqrt{\pi}\Gamma[gD]}} \frac{1}{[\cosh(z/D)]^{gD}} = \frac{\mathcal{N}_K}{[\cosh(z/D)]^{gD}}. \quad (2.15)$$

---

<sup>2</sup>In the simpler case of [11], these were single-component and real.

The equation for  $\chi_1$  is that of a right-handed chiral fermion. Depending on the value of  $g$  whole towers of such localised modes exist but we found that even the second mode contributes at most  $\simeq 10$  percent [11]. We will here restrict our attention to the lowest mode (2.15) only.

We follow the standard quantization procedure and expand the component  $\chi_1$  in terms of plane waves along the domain wall,

$$\chi_1(t, \underline{x}) = \int \frac{d^3 \underline{p}}{(2\pi)^3} \frac{1}{2\omega_p} \left[ b(\underline{p}) e^{i p x} U(\underline{p}) + d^\dagger(\underline{p}) e^{-i p x} V(\underline{p}) \right], \quad (2.16)$$

where we require that

$$p^0 = \omega_p > 0 \quad |\omega_p| = |\underline{p}|. \quad (2.17)$$

The first and second terms in the expansion correspond to positive and negative energy modes respectively. Substituting this into the equation of motion for  $\chi_1$  we find,

$$b(-\underline{p}) [1 + \hat{\underline{p}} \cdot \underline{\sigma}] U(-\underline{p}) e^{-i \omega t} - d^\dagger(\underline{p}) [1 - \hat{\underline{p}} \cdot \underline{\sigma}] V(\underline{p}) e^{i \omega t} = 0, \quad (2.18)$$

with  $\hat{\underline{p}} = \underline{p}/\omega_p$ . The two terms must vanish independently, and so

$$\hat{\underline{p}} \cdot \underline{\sigma} V(\underline{p}) = V(\underline{p}), \quad \hat{\underline{p}} \cdot \underline{\sigma} U(-\underline{p}) = -U(-\underline{p}), \quad (2.19)$$

from which we see that

$$V(\underline{p}) = U(\underline{p}). \quad (2.20)$$

So for instance if we have  $\underline{p} = (0, 0, 1)$ , then

$$U(\underline{p}) \propto \begin{pmatrix} 1 \\ 0 \end{pmatrix}, \quad p^0 > 0, \quad U(\underline{p}) \propto \begin{pmatrix} 0 \\ 1 \end{pmatrix}, \quad p^0 < 0. \quad (2.21)$$

We have therefore that

$$\chi_1(t, \underline{x}) = \int \frac{d^3 \underline{p}}{(2\pi)^3} \frac{1}{2\omega_p} \left[ b(\underline{p}) e^{i p x} U(\underline{p}) + d^\dagger(\underline{p}) e^{-i p x} U(\underline{p}) \right], \quad (2.22)$$

where we choose the normalization

$$U^\dagger(\underline{p}) U(\underline{p}) = 2\omega_p. \quad (2.23)$$

This last relation fixes the normalization of the operators  $b$  and  $d$  so that, given

$$\Psi(t, \underline{x}, z) = \mathcal{F}_K(t, z) \begin{pmatrix} 0 \\ i\chi_1(t, \underline{x}) \end{pmatrix}, \quad \int dz \mathcal{F}_K^*(t, z) \mathcal{F}_K(t, z) = 1, \quad (2.24)$$

the canonical commutation relations

$$\{\Psi_\alpha(t, \underline{x}, z), \Psi_\beta^\dagger(t, \underline{x}', z')\} = \delta_{\alpha\beta} \delta(\underline{x} - \underline{x}') \delta(z - z'), \quad (2.25)$$

reduce to

$$\{\chi_{1\alpha}(t, \underline{x}), \chi_{1\beta}^\dagger(t, \underline{x}')\} = \delta_{\alpha\beta} \delta(\underline{x} - \underline{x}'), \quad (2.26)$$

and

$$\{b(\underline{p}), b^\dagger(\underline{p}')\} = \{d(\underline{p}), d^\dagger(\underline{p}')\} = (2\pi)^3 2\omega_p \delta(\underline{p} - \underline{p}'). \quad (2.27)$$

We will consider moving kinks, incoming or outgoing with a velocity  $v$ , the profile of which are found by applying the appropriate boost to the static solution (2.11),

$$\phi_v(t, \underline{x}, z) = \tanh(\gamma(z - z_0 - vt)/D), \quad (2.28)$$

and correspondingly for the fermion modes

$$\psi_1^v(t, \underline{x}, z) = \sqrt{\frac{\gamma+1}{2}} \mathcal{F}_K(\gamma[z - z_0 - vt]) \chi_1(\gamma[t - v(z - z_0)], \underline{x}), \quad (2.29)$$

$$\psi_2^v(t, \underline{x}, z) = \frac{v\gamma}{\gamma+1} \psi_1^v(t, \underline{x}, z). \quad (2.30)$$

## 2.2 The boundary and more fermion bound states

The boundary action (2.2) leads to the boundary conditions

$$\partial_z \phi|_{z=0} = -\sqrt{\frac{\lambda}{2}} (\phi^2 - 1)|_{z=0}, \quad (2.31)$$

$$\psi_1|_{z=0} = 0. \quad (2.32)$$

These were dubbed  $-BC$  boundary conditions in [11] (see also [15]). Importantly, the static (but not the boosted) kink profile satisfies the boundary condition, and the kink can hence “go into” the wall as it is reflected. Energy is conserved with the reflected kink having (almost) equal and opposite velocity to the incoming one, with only a small amount of kinetic energy lost to scalar radiation. Fig. 1 shows the kink profile as it hits the boundary (left) and the evolution of the scalar at the boundary for various choices of the incident velocity (right). Unsurprisingly, for larger velocity the kink penetrates further into the wall before bouncing back.

When including the boundary action term (2.2) it is energetically favourable for the scalar field to take on the value 1 (rather than  $-1$ ) at the boundary [11], and we take this as the initial condition. This is consistent with a kink incoming from the left, which also has  $\phi(z=0) \simeq 1$ .

As well as the kink, the boundary also carries localised fermion modes and we perform the decomposition

$$\psi_1(t, \underline{x}, z) = 0, \quad \psi_2(t, \underline{x}, z) = \mathcal{F}_B(t, z) \chi_2(t, \underline{x}). \quad (2.33)$$

If the kink is far away, then near the boundary we have that  $\phi(z) = 1$ , and the fermion equation of motion reduces to

$$\partial_z \mathcal{F}_B(t, z) - g \mathcal{F}_B(t, z) = 0, \quad (2.34)$$

$$\dot{\chi}_2(t, \underline{x}) - \sigma^j \partial_j \chi_2(t, \underline{x}) = 0. \quad (2.35)$$

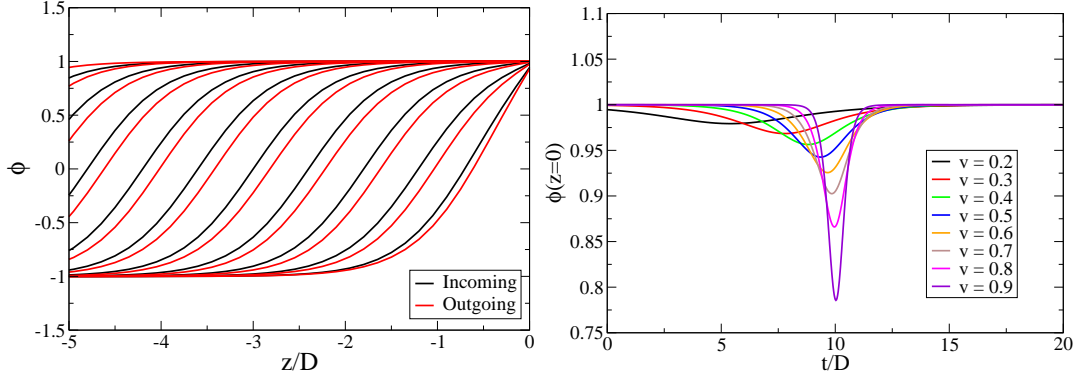


**Figure 1:** Left: The incoming kink profiles before, during and after a kink-boundary collision, for  $v = 0.6$ . Right: The central value  $\phi(t, z = 0)$  for various collision velocities.

which has the (single) solution

$$\mathcal{F}_B(t, z) = \sqrt{g} \exp(gz) = \mathcal{N}_B \exp(gz), \quad (2.36)$$

for the  $z$ -dependence and a left-handed chiral fermion for the boundary field. Note that we are forced to impose the condition  $\psi_1(z = 0) = 0$  in order to find normalisable (and numerically stable) solutions only.

As a result, the boundary modes have opposite helicity to those on the kink, and in order to quantize the system we expand the spinor in terms of these,

$$\chi_2(t, \underline{x}) = \int \frac{d^3 p}{(2\pi)^2} \frac{1}{2\omega_p} \left[ e(\underline{p}) e^{ipx} U(-\underline{p}) + f^\dagger(\underline{p}) e^{-ipx} U(-\underline{p}) \right]. \quad (2.37)$$

### 2.3 Bogoliubov coefficients

For a static kink we have for each mode  $\underline{p}$

$$\Psi^{K^+}(t, \underline{x}, z, \underline{p}) = \frac{\mathcal{N}_K}{[\cosh(z/D)]^{gD}} \begin{pmatrix} 0 \\ e^{ipx} U(\underline{p}) \end{pmatrix}, \quad \Psi^{K^-}(t, \underline{x}, z, \underline{p}) = \frac{\mathcal{N}_K}{[\cosh(z/D)]^{gD}} \begin{pmatrix} 0 \\ i e^{-ipx} U(\underline{p}) \end{pmatrix}, \quad (2.38)$$

and for the boundary

$$\Psi^{B^+}(t, \underline{x}, z, \underline{p}) = \mathcal{N}_B \exp(gz) \begin{pmatrix} e^{ipx} U(-\underline{p}) \\ 0 \end{pmatrix}, \quad \Psi^{B^-}(t, \underline{x}, z, \underline{p}) = \mathcal{N}_B \exp(gz) \begin{pmatrix} e^{-ipx} U(-\underline{p}) \\ 0 \end{pmatrix}. \quad (2.39)$$

In order to quantize the world-volume fields we need to introduce a set of creation/annihilation operators. We consider the system in the asymptotic past, long before the collision, and in the far future, long after the collision. In each of these eras the world volume fields may be expanded in terms of perturbations around the vacuum, as in standard quantum field

theory. As such we write the field operator in the distant past as

$$\begin{aligned}\Psi(t, \underline{x}, z) &= \int \frac{d^3 \underline{p}}{(2\pi)^3} \frac{1}{2\omega_p} \left[ b(\underline{p}) \Psi_{in}^{K+}(t, \underline{x}, z, \underline{p}) + d^\dagger(\underline{p}) \Psi_{in}^{K-}(t, \underline{x}, z, \underline{p}) \right] \\ &+ \int \frac{d^3 \underline{p}}{(2\pi)^3} \frac{1}{2\omega_p} \left[ e(\underline{p}) \Psi_{in}^{B+}(t, \underline{x}, z, \underline{p}) + f^\dagger(\underline{p}) \Psi_{in}^{B-}(t, \underline{x}, z, \underline{p}) \right] \\ &+ \text{bulk continuum modes,}\end{aligned}\tag{2.40}$$

suitably boosted to velocity  $v$ . In this way we find that:  $b^\dagger$  creates positively charged, positive helicity particles on the kink;  $d^\dagger$  creates negatively charged, negative helicity anti-particles on the kink;  $e^\dagger$  creates positively charged, positive helicity particles on the boundary;  $f^\dagger$  creates negatively charged, negative helicity anti-particles on the boundary. We shall not be concerned with the bulk continuum modes.

We then let the kink collide with the boundary and move away again. The resulting fermion field operator can then be re-expanded (in the asymptotic future) in terms of the same modes, boosted in the opposite direction<sup>3</sup>

$$\Psi(t, \underline{x}, z) = \int \frac{d^3 \underline{p}}{(2\pi)^3} \frac{1}{2\omega_p} \left[ \tilde{b}(\underline{p}) \Psi_{out}^{K+}(t, \underline{x}, z, \underline{p}) + \tilde{d}^\dagger(\underline{p}) \Psi_{out}^{K-}(t, \underline{x}, z, \underline{p}) \right]\tag{2.41}$$

$$+ \int \frac{d^3 \underline{p}}{(2\pi)^3} \frac{1}{2\omega_p} \left[ \tilde{e}(\underline{p}) \Psi_{out}^{B+}(t, \underline{x}, z, \underline{p}) + \tilde{f}^\dagger(\underline{p}) \Psi_{out}^{B-}(t, \underline{x}, z, \underline{p}) \right]\tag{2.42}$$

$$+ \text{bulk continuum modes.}\tag{2.43}$$

By comparing the  $e^{ip \cdot x}$  and  $U$  dependence of the initial and final states we find that the two are related through Bogoliubov coefficients  $\alpha_i, \beta_i$  as

$$\Psi_{in}^{K+}(t, \underline{x}, z, \underline{p}) = \alpha_{K+}(\underline{p}) \Psi_{out}^{K+}(t, \underline{x}, z, \underline{p}) + \beta_{K+}(\underline{p}) \Psi_{out}^{B-}(t, \underline{x}, z, -\underline{p}) + b.c.m.,\tag{2.44}$$

$$\Psi_{in}^{K-}(t, \underline{x}, z, \underline{p}) = \alpha_{K-}(\underline{p}) \Psi_{out}^{K-}(t, \underline{x}, z, \underline{p}) + \beta_{K-}(\underline{p}) \Psi_{out}^{B+}(t, \underline{x}, z, -\underline{p}) + b.c.m.,\tag{2.45}$$

$$\Psi_{in}^{B+}(t, \underline{x}, z, \underline{p}) = \alpha_{B+}(\underline{p}) \Psi_{out}^{B+}(t, \underline{x}, z, \underline{p}) + \beta_{B+}(\underline{p}) \Psi_{out}^{K-}(t, \underline{x}, z, -\underline{p}) + b.c.m.,\tag{2.46}$$

$$\Psi_{in}^{B-}(t, \underline{x}, z, \underline{p}) = \alpha_{B-}(\underline{p}) \Psi_{out}^{B-}(t, \underline{x}, z, \underline{p}) + \beta_{B-}(\underline{p}) \Psi_{out}^{K+}(t, \underline{x}, z, -\underline{p}) + b.c.m..\tag{2.47}$$

where we have neglected contributions from the bulk continuum modes and any additional localised excited modes. Given that the mode functions are orthonormal we see that the coefficients are then simply the overlaps of the mode functions, for instance

$$\alpha_{K+}(p, t) = \int dz d^3 x \left( \Psi_{out}^{K+}(t, \underline{x}, z, \underline{p}) \right)^\dagger \Psi_{in}^{K+}(t, \underline{x}, z, \underline{p}).\tag{2.48}$$

We have that

$$\tilde{b}(\underline{p}) = \alpha_{K+}(\underline{p}) b(\underline{p}) + \beta_{B-}(-\underline{p}) f^\dagger(-\underline{p}),\tag{2.49}$$

$$\tilde{d}(\underline{p}) = \alpha_{K-}^*(\underline{p}) d(\underline{p}) + \beta_{B+}^*(-\underline{p}) e^\dagger(-\underline{p}),\tag{2.50}$$

$$\tilde{e}(\underline{p}) = \alpha_{B+}(\underline{p}) e(\underline{p}) + \beta_{K-}(-\underline{p}) d^\dagger(-\underline{p}),\tag{2.51}$$

$$\tilde{f}(\underline{p}) = \alpha_{B-}^*(\underline{p}) f(\underline{p}) + \beta_{K+}^*(-\underline{p}) b^\dagger(-\underline{p}).\tag{2.52}$$

---

<sup>3</sup> $\Psi_{in} = \Psi(v_{in}), \Psi_{out} = \Psi(v_{out})$ , where in practice we determine  $v_{out}$  from the evolution of the kink. We find that  $v_{out} = -v_{in}$  to within  $10^{-3}$ .



The mode functions are all normalised which means that if the bulk modes are negligible Bogoliubov coefficients relating the bound-state modes form a unitary matrix. This implies that

$$|\alpha_{K-}|^2 \simeq |\alpha_{B+}|^2, \quad |\alpha_{B-}|^2 \simeq |\alpha_{K+}|^2, \quad (2.53)$$

$$|\beta_{K-}|^2 \simeq |\beta_{B+}|^2, \quad |\beta_{B-}|^2 \simeq |\beta_{K+}|^2. \quad (2.54)$$

The final particle number in for instance the  $K+$  mode can then be found in terms of the particle numbers in the initial state

$$\begin{aligned} (2\pi)^3 2\omega_p n^{K+}(p) \delta^3(p-q) &= \langle \tilde{b}(\underline{p})^\dagger \tilde{b}(\underline{q}) \rangle \\ &= \langle \left( \alpha_{K+}(\underline{p}) b(\underline{p}) + \beta_{B-}(-\underline{p}) f^\dagger(-\underline{p}) \right)^\dagger \left( \alpha_{K+}(\underline{q}) b(\underline{q}) + \beta_{B-}(-\underline{q}) f^\dagger(-\underline{q}) \right) \rangle \end{aligned} \quad (2.55)$$

The expectation number of the particle operator then depends on the choice of initial quantum state. If we suppose that the state before the collision is in the vacuum of the  $b$ ,  $d$ ,  $e$ ,  $f$  operators then we see that the spectrum of particles after the collision is given by

$$n^{K+}(p) = |\beta_{B-}(p)|^2, \quad (2.56)$$

$$n^{K-}(p) = |\beta_{B+}(p)|^2, \quad (2.57)$$

$$n^{B+}(p) = |\beta_{K-}(p)|^2, \quad (2.58)$$

$$n^{B-}(p) = |\beta_{K+}(p)|^2. \quad (2.59)$$

All that remains now is the calculation of the Bogoliubov coefficients, for this we need to solve the Dirac equation.

## 2.4 Individual modes

As the equations of motion are linear, we can consider each mode separately. For a given  $\underline{p}$  we have

$$\psi_1(t, \underline{x}, z, \underline{p}) = e^{i\underline{p}\underline{x}} \tilde{\psi}_1(t, z, \underline{p}) U(\underline{p}), \quad \psi_2(t, \underline{x}, z, \underline{p}) = e^{i\underline{p}\underline{x}} \tilde{\psi}_2(t, z, \underline{p}) U(\underline{p}). \quad (2.60)$$

Then the equations of motion give us

$$\dot{\tilde{\psi}}_1(t, z, \underline{p}) + i|\underline{p}|\tilde{\psi}_1(t, z, \underline{p}) + \partial_z \tilde{\psi}_2(t, z, \underline{p}) - g\phi(t, z)\tilde{\psi}_2(t, z, \underline{p}) = 0, \quad (2.61)$$

$$\dot{\tilde{\psi}}_2(t, z, \underline{p}) - i|\underline{p}|\tilde{\psi}_2(t, z, \underline{p}) + \partial_z \tilde{\psi}_1(t, z, \underline{p}) + g\phi(t, z)\tilde{\psi}_1(t, z, \underline{p}) = 0, \quad (2.62)$$

where we have used (2.19)

$$\underline{p} \cdot \underline{\sigma} U(\underline{p}) = |\underline{p}| \hat{p} \cdot \underline{\sigma} U(\underline{p}) = |\underline{p}| U(\underline{p}). \quad (2.63)$$

We solve the equations of motion numerically, starting from the initial condition of an incoming boosted kink and the appropriate fermion bound state

$$\tilde{\psi}_1 = \sqrt{\frac{\gamma+1}{2}} \exp[i\omega\gamma v(z-z_0)] \frac{\mathcal{N}_K}{[\cosh(\gamma(z-z_0))]^{gD}}, \quad (2.64)$$

$$\tilde{\psi}_2 = \frac{v\gamma}{\gamma+1} \tilde{\psi}_1, \quad (2.65)$$

for the kink mode and

$$\tilde{\psi}_1 = 0, \quad (2.66)$$

$$\tilde{\psi}_2 = \mathcal{N}_B \exp(gz), \quad (2.67)$$

for the boundary mode. Then after the simulation has run its course we reexpand on the same modes, but boosted with the velocity of the outgoing kink as described above. This gives us the Bogoliubov coefficients.

This covers the positive energy modes  $\Psi^+$  (2.38)(2.39). The negative energy modes  $\Psi^-$  (2.38)(2.39) lead to eqs. (2.61), (2.62) with  $|p| \rightarrow -|p|$ , which amounts to complex conjugating the equation of motion, so we should find that  $|\alpha_{K+}| = |\alpha_{K-}|$ ,  $|\beta_{K+}| = |\beta_{K-}|$ ,  $|\alpha_{B+}| = |\alpha_{B-}|$ ,  $|\beta_{B+}| = |\beta_{B-}|$ . We checked numerically that this is indeed the case, and so in the following we shall only quote the absolute values  $|\alpha_K|^2$ ,  $|\alpha_B|^2$ ,  $|\beta_K|^2$ ,  $|\beta_B|^2$ .

### 3. The fermion spectrum

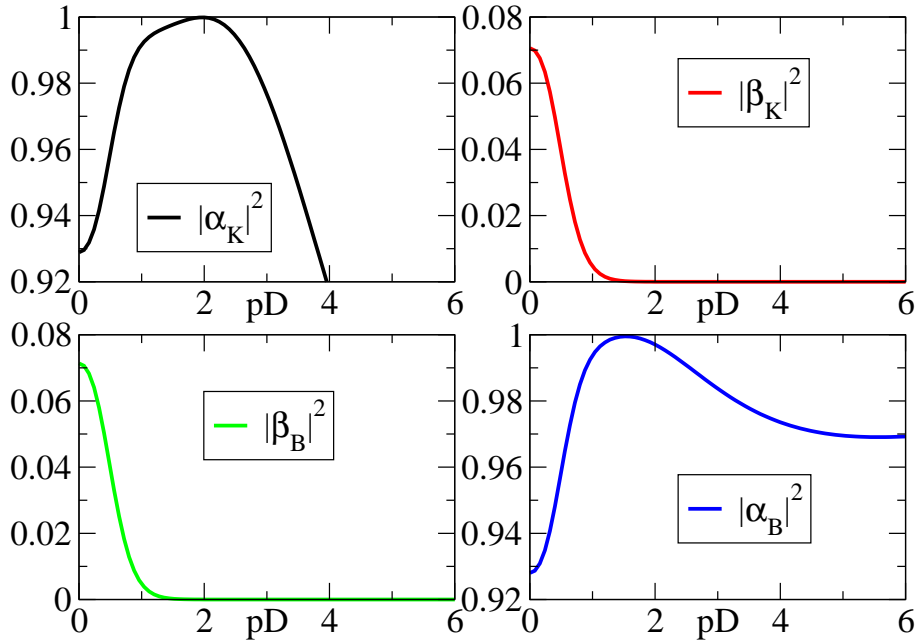


**Figure 2:** The  $p$ -dependence of the Bogoliubov coefficients; of a mode on itself  $|\alpha_{K,B}|^2$ , and transferred from one mode to another  $|\beta_{K,B}|^2$ .  $v = 0.6$ ,  $g = 2$ .

We show in Fig. 2 the  $p$ -dependence of the various Bogoliubov coefficients. In this example, the incident velocity  $v$  is 0.6 and the coupling  $g$  is 2. Throughout the simulations, we use  $\lambda = 2$ ,  $D = 1$ .

If there were no bulk modes, nor any extra excited world-volume modes, we would have that  $|\alpha_K|^2 + |\beta_K|^2 = 1 = |\alpha_B|^2 + |\beta_B|^2$ . Therefore, what Fig. 2 is telling us is that for  $pD \lesssim 2$  there is very little excitation of the bulk modes, but for higher momenta the bulk modes become more important. This is to be expected given that the mass gap for

the bulk fermions is  $g$  (where we have the  $|\phi|_{bulk} = 1$ ), which for the simulation of Fig. 2 was  $g = 2$ . Now recall from (2.56)-(2.59) that the  $\beta$  coefficients give us the particle spectrum for the world-volume fields, if they are in the vacuum state before the collision. We see that the spectrum is peaked around zero world-volume momentum, with a width in momentum-space given by the inverse of the wall width,  $D$ .

### 3.1 Large $p$

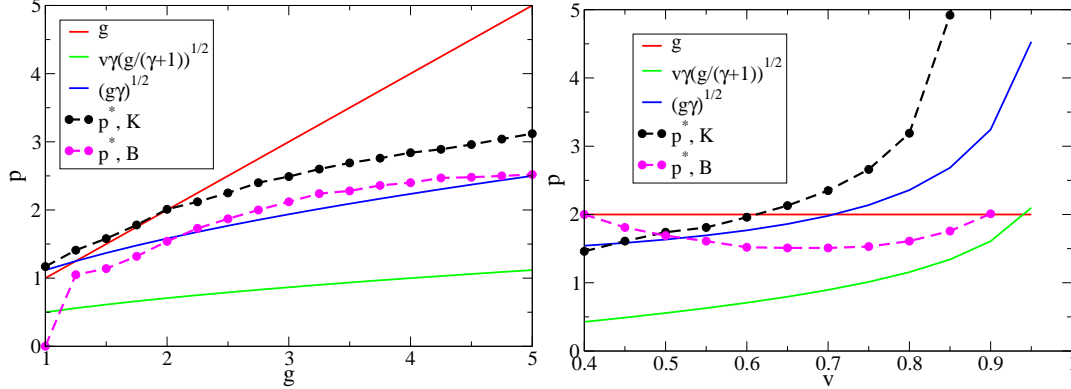


**Figure 3:** The momentum  $p^*$  for which the fermions start to fall off the kink, compared to simple estimates.  $g$ -dependence (left) and  $v$  dependence (right).

We can understand the behaviour in Fig. 2 by rewriting the equations of motion (2.61), (2.62) as second order differential equations, to find

$$\begin{aligned}\ddot{\tilde{\psi}}_1(t, z) &= \partial_z^2 \tilde{\psi}_1(t, z) - (p^2 + g^2 \phi(t, z)) \tilde{\psi}_1(t, z) + g \left( \dot{\phi} \tilde{\psi}_2(t, z) + \partial_z \phi \tilde{\psi}_1(t, z) \right), \\ \ddot{\tilde{\psi}}_2(t, z) &= \partial_z^2 \tilde{\psi}_2(t, z) - (p^2 + g^2 \phi(t, z)) \tilde{\psi}_2(t, z) - g \left( \dot{\phi} \tilde{\psi}_1(t, z) + \partial_z \phi \tilde{\psi}_2(t, z) \right).\end{aligned}\quad (3.1)$$

The localisation of the fermion modes is due to the decrease in  $\phi(z)$  and hence mass within the kink. Clearly, when  $p^2$  dominates  $g^2 \phi^2$  as well as the other terms on the right hand side, the localisation will not be as manifest.

We can estimate when this will happen by comparing  $p^2$  to the size of the other terms. In the kink background, we can use (2.28)(2.29)(2.30) to write

$$g^2 \phi^2 \tilde{\psi}_1 < g^2 \tilde{\psi}, \quad g \dot{\phi} \tilde{\psi}_1 < \frac{gv^2 \gamma^2}{\gamma + 1} \tilde{\psi}_2, \quad g \partial_z \phi \tilde{\psi}_1 < g \gamma \tilde{\psi}_1. \quad (3.2)$$

Hence, we expect the  $p^2$  term in (3.1) to dominate when

$$p > g, \quad p > \sqrt{g} \frac{c\gamma}{\sqrt{\gamma + 1}}, \quad p > \sqrt{g\gamma}. \quad (3.3)$$

Fig. 3 (left) shows the  $p$  value at which the modes start to “fall off” ( $p^*$ ) plotted against  $g$ , for  $v = 0.6$ . This quantity  $p^*$  is found from the simulations by observing where  $|\alpha_K|$  starts to decrease. Keeping in mind to allow for an overall factor, the functional dependence of  $p^*$  is best reproduced by the  $\sqrt{g\gamma}$  line, originating from the spatial derivative term in

(3.1). The  $p^*$  derived from the  $K$  and  $B$  modes are also roughly compatible. In Fig. 3 (right) we fix  $g$  and show the dependence on  $v$ . Again, the behaviour of the  $K$  mode  $p^*$  is roughly described by the  $\sqrt{g\gamma}$ -dependence. When taking  $p^*$  from the  $B$  mode, however, we observe a somewhat different dependence. Still, we believe we understand qualitatively the behaviour of the spectrum at high  $p$ . Our main focus will be the transfer between  $B$  and  $K$  modes, which manifests itself at small  $p$ .

### 3.1.1 Velocity dependence

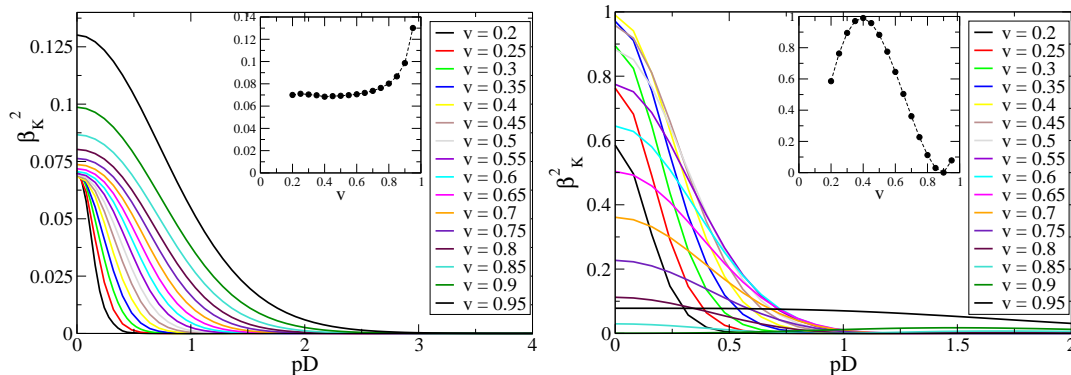


**Figure 4:** The velocity dependence of the  $|\beta_{K,B}|$ -spectrum for  $g = 2$  (left) and  $g = 4$  (right). Overlaid the  $v$ -dependence of the  $p = 0$  mode.

As the incident velocity is increased, the amplitude of the  $\phi(z = 0)$  dip at the collision (Fig. 1, right) increases as the kink is able to penetrate deeper into the wall. This has a significant impact on the fermion spectrum, as can be seen in Fig. 4. For  $g = 2$ , the width of the distribution increases as  $v$  goes from 0.2 to 0.5, beyond which also the amplitude starts to grow. We note that this is simply the behaviour of the zero-mode [12, 11]. For  $g = 4$  the picture becomes somewhat more complicated, in that for  $v < 0.4$ , the distribution grows and widens, but then shrinks back to very small values for  $v > 0.4$ . Hence simple kinematics does not explain the behaviour. The dependence on  $v$  is oscillatory rather than monotonic.

### 3.1.2 Coupling dependence

We now fix the velocity and vary the coupling  $g$ . In [11] we found that the  $k = 0$  mode has an oscillatory dependence on  $g$ , with amplitude and phase somewhat dependent on  $v$ . In Fig. 5 (left) we see the spectra for  $v = 0.4$  at various values of  $g$ . The overlay shows the zero-mode oscillation, and to a good approximation, the spectra are almost Gaussian with the zero mode setting the amplitude. The width has a separate dependence on  $g$ .

In Fig. 5 (right) we show the result when fixing  $v$  to 0.9. Again, we overlay the zero mode result, which sets the amplitude. But now the spectrum is (at least for  $g > 3$ ) a non-monotonic function of  $p$ , with maximum away from  $p = 0$ . Again, the width has a separate dependence on  $g$ , but whereas for  $v = 0.4$  the trend is for the width to shrink with amplitude, for  $v = 0.9$  the opposite is the case. Note also the overall difference in vertical and horizontal scale between the two figures.

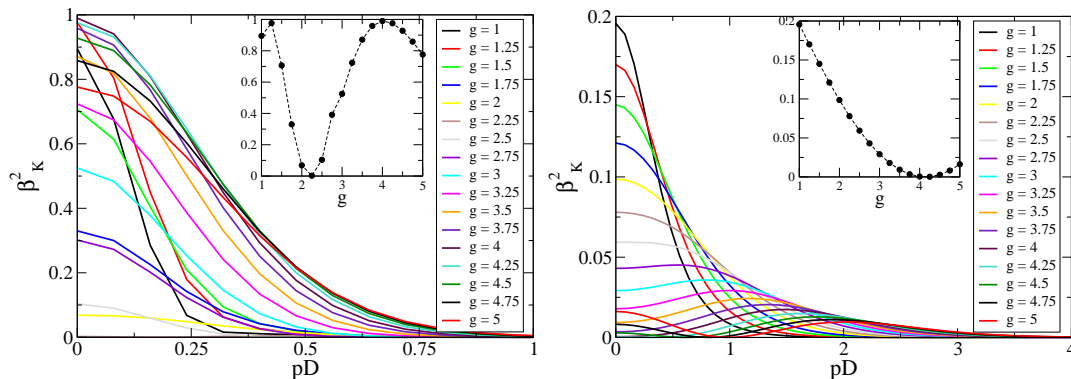


**Figure 5:** The coupling dependence of the  $|\beta_{K,B}|$ -spectrum for  $v = 0.4$  (left) and  $v = 0.9$  (right). Overlaid the  $g$ -dependence of the  $p = 0$  mode. Note the different  $p$ -ranges in the two plots.

#### 4. Conclusion

Our purpose was to model the particle creation event, as observed by someone on either brane or boundary, due to the collision between brane and boundary. We have extended the work of [11] by including fermions with momentum in the braneworld directions.

We found that a non-trivial fermion spectrum emerges, in general strongly centered around  $p = 0$  but at high incident velocities it becomes peaked away from zero momentum. The oscillatory dependence, reported in [12, 11], of the zero momentum coefficients on scalar-fermion coupling  $g$  and velocity  $v$  extends to finite  $p$ . The zero-mode sets the amplitude of the spectrum, with the width having its own dependence on  $v$  and  $g$ . In the previous study we included an excited zero momentum bound state as well as the ground state, there we found that this mode had little impact on the ground state fermion [11]. In principle there will also be excited modes with non-zero braneworld momentum. While the previous study reveals that such modes have little impact for low momentum, they may play a more significant role at higher momentum

Generalising to more complicated scalar potentials and hence different domain wall profiles is straightforward, although one may run into trouble when solving analytically for the bound states. If so these can simply be found numerically. Such a system has been analyzed for the matter sector of the standard model [7], although braneworld gauge fields remain problematic. With the addition of extra fields we would expect the spectrum of braneworld particles to thermalize, eventually reaching an equilibrium distribution.

A natural further extension of this work would be to include multiple scalar fields (complex,  $SU(2)$  doublets) and allow for  $C$  and  $CP$  symmetry breaking. This of course would be relevant for baryogenesis models, where branes deposit asymmetric amounts of matter and anti-matter on the world brane.

In 3+1 dimensions, similar methods may also be employed specifically for electroweak baryogenesis, by interpreting the kink as an advancing bubble wall and calculating reflection and transmission coefficients for fermions hitting or being hit by the  $CP$ -violating wall. We would then have to consider a finite temperature state of fermions, and possibly include gauge fields in the background in addition to the scalar domain wall.

## Acknowledgments

P.M.S is supported by STFC and A.T. is supported by STFC Special Programme Grant “*Classical Lattice Field Theory*”. We gratefully acknowledge the use of the UK National Cosmology Supercomputer, Cosmos, funded by STFC, HEFCE and Silicon Graphics.

## References

- [1] C. V. Johnson, *Cambridge, USA: Univ. Pr. (2003) 548 p*
- [2] P. Horava and E. Witten, Nucl. Phys. B **475**, 94 (1996) [arXiv:hep-th/9603142].
- [3] V. A. Rubakov and M. E. Shaposhnikov, Phys. Lett. B **125**, 136 (1983).
- [4] A. J. Niemi and G. W. Semenoff, Phys. Rept. **135**, 99 (1986).
- [5] R. Jackiw and C. Rebbi, Phys. Rev. D **13**, 3398 (1976).
- [6] R. Jackiw and P. Rossi, Nucl. Phys. B **190**, 681 (1981).
- [7] R. R. Volkas, arXiv:0708.3884 [hep-ph].
- [8] G. R. Dvali and M. A. Shifman, Phys. Lett. B **396** (1997) 64 [Erratum-ibid. B **407** (1997) 452] [arXiv:hep-th/9612128].
- [9] J. Khoury, B. A. Ovrut, P. J. Steinhardt and N. Turok, Phys. Rev. D **64** (2001) 123522 [arXiv:hep-th/0103239].
- [10] Y. i. Takamizu and K. i. Maeda, Phys. Rev. D **70**, 123514 (2004) [arXiv:hep-th/0406235].
- [11] P. M. Saffin and A. Tranberg, arXiv:0705.3606 [hep-th].
- [12] G. Gibbons, K. i. Maeda and Y. i. Takamizu, Phys. Lett. B **647** (2007) 1 [arXiv:hep-th/0610286].
- [13] G. Aarts and J. Smit, Nucl. Phys. B **555** (1999) 355 [arXiv:hep-ph/9812413].
- [14] S. Randjbar-Daemi and M. E. Shaposhnikov, Phys. Lett. B **492** (2000) 361 [arXiv:hep-th/0008079].
- [15] N. D. Antunes, E. J. Copeland, M. Hindmarsh and A. Lukas, Phys. Rev. D **69** (2004) 065016 [arXiv:hep-th/0310103].